

Concussive Brain Trauma in the Mouse Results in Acute Cognitive Deficits and Sustained Impairment of Axonal Function

Jennifer A. Creed,¹ Ann Mae DiLeonardi,¹ Douglas P. Fox,²
Alan R. Tessler,^{2,3} and Ramesh Raghupathi^{1,2}

Abstract

Concussive brain injury (CBI) accounts for approximately 75% of all brain-injured people in the United States each year and is particularly prevalent in contact sports. Concussion is the mildest form of diffuse traumatic brain injury (TBI) and results in transient cognitive dysfunction, the neuropathologic basis for which is traumatic axonal injury (TAI). To evaluate the structural and functional changes associated with concussion-induced cognitive deficits, adult mice were subjected to an impact on the intact skull over the midline suture that resulted in a brief apneic period and loss of the righting reflex. Closed head injury also resulted in an increase in the wet weight:dry weight ratio in the cortex suggestive of edema in the first 24 h, and the appearance of Fluoro-Jade-B-labeled degenerating neurons in the cortex and dentate gyrus of the hippocampus within the first 3 days post-injury. Compared to sham-injured mice, brain-injured mice exhibited significant deficits in spatial acquisition and working memory as measured using the Morris water maze over the first 3 days ($p < 0.001$), but not after the fourth day post-injury. At 1 and 3 days post-injury, intra-axonal accumulation of amyloid precursor protein in the corpus callosum and cingulum was accompanied by neurofilament dephosphorylation, impaired transport of Fluoro-Gold and synaptophysin, and deficits in axonal conductance. Importantly, deficits in retrograde transport and in action potential of myelinated axons continued to be observed until 14 days post-injury, at which time axonal degeneration was apparent. These data suggest that despite recovery from acute cognitive deficits, concussive brain trauma leads to axonal degeneration and a sustained perturbation of axonal function.

Key words: axonal injury; axonal transport; compound action potential; concussion; spatial learning; traumatic brain injury; working memory

Introduction

CONCUSSIVE BRAIN INJURY (CBI) accounts for approximately 75% of all brain-injured people in the United States each year, and is particularly prevalent in contact sports (Bazarian et al., 2005; Ropper and Gorson, 2007). The diagnosis of concussion is based on a rapid onset of impaired neurologic function such as loss of balance and amnesia (McCrory et al., 2009). Although 80–90% of concussions resolve spontaneously within 10 days, some functional deficits persist for weeks to years (Geurts et al., 1999; McCrea et al., 2003). Impaired cognitive functions include loss of concentration, deficits in working memory, and reduced speed of processing (Levin et al., 1987; McCrory et al., 2009). In this regard, concussed patients demonstrate lower scores in verbal

and visual memory tasks (Lovell et al., 2003, 2004; Maddocks and Saling, 1996), and information processing (Hinton-Bayre et al., 1999; Niogi et al., 2008), and impaired attention (Kraus et al., 2007). Although standard neuroimaging fails to identify structural abnormalities, diffusion tensor imaging can detect axonal injury (Arfanakis et al., 2002; Niogi et al., 2008; Smits et al., 2010; Wilde et al., 2008). These imaging findings have been supported by post-mortem examination of several cases of concussed brains demonstrating abnormal axonal morphology and disrupted axonal transport (Blumbergs et al., 1994).

Experimental models of CBI, using either fluid-percussion or weight-drop injury in rats and cats, traditionally have been defined by brief periods of apnea, suppression of electrical brain activity, and loss of pressure autoregulation (Dixon

¹Program in Neuroscience, ²Department of Neurobiology and Anatomy, Drexel University College of Medicine, and ³Veteran's Administration Medical Center, Philadelphia, Pennsylvania.

et al., 1987; Foda and Marmarou, 1994; Hamm, 2001; Yamaki et al., 1994), ionic dyshomeostasis such as increased extracellular potassium (Katayama et al., 1990), and prolonged calcium accumulation (Fineman et al., 1993), as well as changes in patterns of regional glucose utilization (Hovda et al., 1990; Yoshino et al., 1991). Accompanying these acute alterations were intra-axonal swellings characterized by the presence of compacted neurofilaments and disrupted microtubules, leading to accumulation of organelles and vesicles containing β -amyloid precursor protein (β -APP) (Buki and Povlishock, 2006; Foda and Marmarou, 1994; Lewen et al., 1995; Povlishock et al., 1983; Stone et al., 2000). Moreover, both myelinated and unmyelinated axons within the corpus callosum exhibited reduced compound action potentials (CAPs) up to a week after injury (Baker et al., 2002; Reeves et al., 2005) indicative of functional deficits. However, behavioral analysis in brain-injured animals revealed acute (within 3 days) and chronic (up to 1 month) deficits in vestibulomotor and cognitive function (Hamm, 2001; Tang et al., 1997a; Yamaki et al., 1997; Zohar et al., 2003), along with post-concussive syndrome (Ryan and Warden, 2003; Williams et al., 2010).

Diffuse traumatic brain injury (TBI), including CBI, has been modeled in mice (Laurer et al., 2001; Longhi et al., 2005; Spain et al., 2010; Tang et al., 1997a, 1997b; Zohar et al., 2003). Injury induced by a weight-drop, fluid-percussion, or a modified cortical impact device resulted in diffuse neurodegeneration in the cortex and hippocampus, and β -APP-positive intra-axonal swellings in the thalamus, corpus callosum, and external capsule (Longhi et al., 2005; Spain et al., 2010; Tang et al., 1997b; Tashlykov et al., 2007). As was observed in rats, closed head injury in mice resulted in long-term behavioral dysfunction characterized by learning deficits, depressive behavior, and increased passive avoidance (Milman et al., 2005; Spain et al., 2010; Tang et al., 1997a; Zohar et al., 2003). In contrast, impact to the intact skull using a silicone-tipped indenter only resulted in a transient deficit in motor function with no effect on spatial learning ability (Laurer et al., 2001; Longhi et al., 2005). While these animal models reflect the acute neurochemical, microscopic, and anatomical pathophysiology of concussive brain trauma, they do not appear to model the hallmark of concussion: transient neurologic (cognitive) dysfunction. With this in mind, we developed a model of closed head injury in mice using a cortical impact device in a manner similar to previously published studies in immature rats (DiLeonardi et al., 2009; Huh et al., 2008).

In this report, we demonstrate that impact to the intact skull over the midline suture between the lambda and bregma sutures resulted in spatial learning and working memory deficits only in the first 3 days after trauma, which were resolved by day 4 post-injury. Axonal swellings in the corpus callosum containing APP, dephosphorylated neurofilament, or synaptophysin, were observed up to 3 days post-injury, as well as degenerating axons at 14 days post-injury. These structural alterations in injured axons were accompanied by functional deficits that manifested as reductions in CAPs and decreased retrograde transport which were present up to 2 weeks post-injury. In addition to alterations in the white matter, the cortex underlying the impact site was edematous over the first 24 h post-injury and contained Fluoro-Jade-B-positive neurons. Neuronal degeneration was also observed within the hilus of the dentate gyrus up to 3 days post-injury.

Collectively, these observations are indicative of the ongoing degeneration of the concussed brain despite resolution of cognitive deficits.

Methods

Animals

Adult male C57BL/6J mice (18–35 g; Jackson Laboratories, Bar Harbor, ME) were used for this study (Table 1). Mice were given standard lab chow and water *ad libitum*, and maintained in a controlled temperature environment with a 12-h light-dark cycle. All procedures used followed the guidelines set by the U.S. Public Health Service Policy on Humane Care and Use of Laboratory Animals, and the National Institutes of Health (NIH) Guide for the Care and Use of Laboratory Animals, and were approved by the Drexel University Institutional Animal Care and Use Committee.

Concussive brain injury

Mice were subjected to closed head injury in a manner similar to that used in immature rats (Huh et al., 2008). Anesthesia was induced with isoflurane (1.5%; Webster Veterinary, Sterling, MA) inhalation via a nose cone, and the corneas were kept moist during surgery by applying Lubricants ointment (Bausch and Lomb, Tampa, FL). Body temperature was maintained throughout the entire procedure by using a heating pad at 37°C. The scalp was swabbed with povidone-iodine and a subcutaneous injection of lidocaine was administered prior to making a 1.0-cm midline rostral-to-caudal incision to expose the skull. The periosteum was reflected (Fig. 1A), and the animals were placed in a standard mouse restrainer (Braintree Scientific, Braintree, MA) with the head supported by a soft foam pad to make it level with the body. The restrainer was positioned under the cortical impact device (Custom Design & Fabrication, Richmond, VA), and the 5-mm-diameter hemispheric metal impactor tip was zeroed by touching it to the sagittal suture midway between the bregma and the lambda (Fig. 1B). At 30 sec after removal of anesthesia, the impactor was electronically driven perpendicularly onto the exposed sagittal suture at a velocity of 5.0 m/sec to a depth of 1.5 mm farther than the zero point. Immediately after the impact, the righting reflex was evaluated by measuring the time required for the mice to regain their normal posture over three consecutive attempts when placed in the supine position. The animals were re-anesthetized so that the scalp incision could be closed with 4-0 silk suture. Sham-injured mice were subjected to the same procedures without receiving an impact. All animals were allowed to recover on a heating pad set at 37°C, and upon becoming ambulatory were returned to their home cages.

Corpus callosotomy

Transection of the corpus callosum was performed as previously described (Schalomon and Wahlsten, 1995). Mice ($n=7$) were anesthetized with sodium pentobarbital (65 mg/kg IP) and immobilized in a stereotaxic frame. The scalp was swabbed with povidone-iodine and a subcutaneous injection of lidocaine was administered prior to making a 1.0-cm midline rostral-to-caudal incision to expose the skull. A 5-mm-diameter craniectomy was made over the sagittal suture midway between the bregma and the lambda. The dura

TABLE 1. ACUTE NEUROLOGICAL STATUS RESPONSES FOLLOWING CLOSED HEAD INJURY

Study	Experimental group	n	Apnea (sec)	Righting reflex (sec)	Skull fracture (%)
Histology	Sham	6	0.0±0.0	15.2±5.6	NA
	Injured-24 h	6	25.0±21.0*	154.7±22.9*	100
	Injured-3 days	6	25.3±16.3*	163.7±27.9*	100
	Injured-7 days	6	25.8±19.7*	167.8±31.4*	100
Immunoblot	Sham	4	0.0±0.0	18.5±7.2	NA
	Injured-24 h	4	29.5±19.9*	133.8±33.3*	100
	Injured-3 days	4	37.5±21.0*	155.0±36.3*	100
	Injured-7 days	4	31.3±13.1*	138.8±23.9*	100
Tissue water content	Sham-6 h	6	0.0±0.0	13.2±6.9	NA
	Injured-6 h	9	23.3±15.9*	211.8±44.3*	100
	Sham-48 h	6	0.0±0.0	24.7±7.1	NA
	Injured-48 h	9	31.8±22.4*	181.7±56.8*	100
Retrograde axonal transport	Sham	4	0.0±0.0	18.8±8.5	NA
	Injured-3 days	8	25.0±17.3*	163.4±41.1*	100
	Injured-7 days	8	23.6±11.9*	167.4±13.9*	100
	Injured-14 days	8	22.5±13.9*	144.4±41.4*	100
Spatial learning (days 1–3) and working memory (days 7–9)	Sham	6	0.0±0.0	13.3±2.9	NA
	Injured	9	26.3±32.5*	133.7±27.8*	100
Spatial learning (days 4–6)	Sham	8	0.0±0.0	13.4±2.8	NA
	Injured	9	25.6±15.9*	157.8±29.0*	100
Working memory (days 1–3)	Sham	6	0.0±0.0	17.0±7.0	NA
	Injured	9	31.9±21.2*	189.9±20.5*	100
Compound action potentials	Sham-24 h	6	0.0±0.0	15.3±3.5	NA
	Injured-24 h	6	41.7±35.6*	173.3±60.0*	100
	Sham-14 days	9	0.0±0.0	14.6±4.1	NA
	Injured-14 days	8	20.5±11.5*	140.3±32.0*	100

* $p < 0.05$ compared to study-matched sham animals.

Immediately following impact, mice were evaluated for time of loss of breathing (apnea), righting reflex, and the presence of skull fractures. Separation either by recovery time within a study or across the multiple experiments showed no significant differences in the injured animals for both latency to the righting reflex and the duration of apnea. Apnea, righting reflex, and skull fracture values are presented as the mean±standard deviation.

NA, not applicable.

was removed and an ultra-fine micro-knife (15° cutting angle, 0.15-mm thickness, carbon steel tip; Fine Science Tools, Foster City, CA) secured to a stereotaxic arm was lowered slowly between the two cortical hemispheres at the bregma suture, taking care not to disrupt the sagittal sinus. When the blade reached a depth of 2 mm, it was moved 3 mm in the posterior direction along the sagittal groove. No bleeding was observed, indicating that the vein was not breached. Following the transection, a cranioplasty was glued to the skull using Vetbond, and the scalp incision was closed with 4-0 silk suture. All animals were allowed to recover on a heating pad set

at 37°C, and upon becoming ambulatory were returned to their home cages.

Tissue water content

An increase in tissue water content, an indication of edema, was determined using the wet weight:dry weight method (Dempsey et al., 2000). Briefly, at either 6 or 24 h following surgery or injury, the animals were euthanized using Euthasol® (Virbac AH Inc., Fort Worth, TX) and decapitated. The brain was removed and a 3-mm-thick coronal section

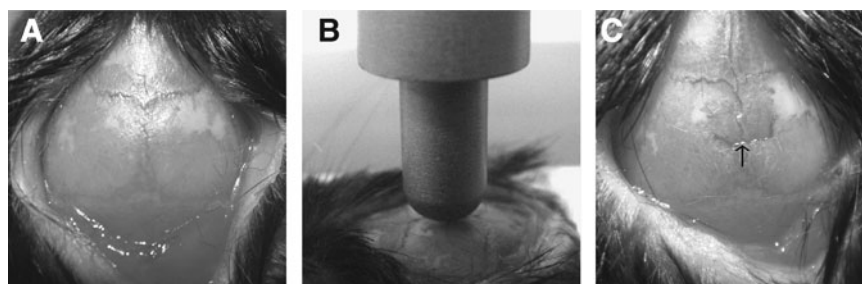


FIG. 1. Model of concussive brain trauma. (A) The skull was exposed by reflecting the periosteum. (B) The hemispheric metal indenter tip was zeroed onto the surface of the skull, centered between the lambda and bregma sutures and over the sagittal suture. (C). Note the location of the minor fracture perpendicular to the sagittal suture typically observed immediately following impact.

representing the area directly below the impact site was isolated and placed on an ice-cold glass plate. The cortex, hippocampus, and thalamus from injured and sham (uninjured) animals were dissected and immediately weighed to obtain the wet weight (WW). The samples were then dried in a convection oven at 70°C for 48 h and weighed to determine the dry weight (DW). Water content was then calculated using the equation: $[(WW - DW)/WW] \times 100$.

Retrograde axonal transport

The neuronal tracer Fluoro-Gold (FG; FluoroChrome Inc., Englewood, CO) was used to assess retrograde axonal transport (Schmued and Fallon, 1986). Mice were anesthetized with sodium pentobarbital (65 mg/kg IP) and immobilized in a stereotaxic frame. The scalp was swabbed with povidone-iodine and a subcutaneous injection of lidocaine was administered prior to making a 1.0-cm midline rostral-to-caudal incision to expose the skull. A hand drill was used to expose the dura above the target site (2.0 mm anteroposterior from the bregma suture, and 2.0 mm mediolateral from the sagittal suture), and FG (1 μ L of a 2% solution in de-ionized water) was manually injected into the cortex (0.5 mm deep from the dura) over 3 min using a 10- μ L gas-tight Hamilton syringe with a beveled tip (0.47 mm outer diameter, 26 gauge; SGE Analytical Science, Austin, TX). To mitigate backflow along the needle track, the needle was left *in situ* for 5 min after the injection. Sham- and brain-injured mice received FG injections at 1, 5, or 12 days following surgery and/or injury, while callosotomy mice were injected with FG immediately after the transection; all mice were euthanized 48 h later. FG-positive cells were counted in three coronal sections (1.46, 1.94, and 2.42 mm posterior to the bregma) in 4 adjacent non-overlapping fields (10 \times magnification) covering the dorsal-ventral cortex in the hemisphere contralateral to the injection site. Values represent the mean number of FG-positive cells across each of the four high-powered fields (HPF) in each of the 3 sections.

Histologic analyses

At 48 h following callosotomy or at 24 h, or 3, 7, and 14 days following CBI or sham-injury, the brains were processed for immunohistochemical and histologic analysis as previously described (Huh et al., 2008; Saatman et al., 2006). One set of 40- μ m-thick coronal sections taken between +1.1 mm and -3.8 mm relative to bregma (10–11 sections/set) was mounted onto gelatin-coated slides and stained with 2% cresyl violet and 0.2% cyanine R (Nissl-myelin). A second set of sections was mounted and stained with Fluoro-Jade-B (Chemicon, Temecula, CA) as previously described (Huh et al., 2008; Tong et al., 2001). All Fluoro-Jade-B-labeled cells in each section were manually counted in the following manner: the total number of Fluoro-Jade-B-positive cells was counted in the cortex (both hemispheres) in each of 8 sections (approximately 480 μ m apart) between 0.86 mm anterior to bregma and 3.4 mm posterior to bregma, and are presented as an arithmetic mean per section. Five coronal sections (480 μ m apart) between 1.34 mm and 3.18 mm posterior to bregma were used to count all Fluoro-Jade-B-positive cells in the hippocampus. Sets of adjacent sections were analyzed for the presence of β -APP, polyclonal antibody to the C-terminus of the protein (1:2000; Zymed, Carlsbad, CA),

dephosphorylated 200-kDa neurofilament protein (1:2500, clone SMI32; Covance, Princeton, NJ), and synaptophysin (1:1000, clone SVP-38; Sigma-Aldrich, St. Louis, MO), using standard procedures (DiLeonardi et al., 2009; Huh et al., 2008; Saatman et al., 2006). As a negative control, one or two sections from each animal were incubated with all reagents except the primary antibodies. APP-immunoreactive profiles were quantified in three coronal sections (1.46, 1.94, and 2.42 mm posterior to bregma) from each brain as previously described (DiLeonardi et al., 2009).

Immunoblot analysis

At 24 h, and 3 and 7 days following CBI or sham-injury, the corpus callosum was dissected on an ice-cold glass plate and placed in buffer (50 mM Tris HCl [pH 8.0], 150 mM NaCl, 2 mM EDTA, 0.1% sodium dodecyl sulfate [SDS], 1% Nonidet P-40, and 0.5% sodium deoxycholate) containing the components of the Complete Roche system and pepstatin A (20 μ g/mL) to inhibit proteases, and 50 mM sodium vanadate to inhibit phosphatases. Tissue samples were sonicated and then centrifuged at 14,000g for 10 min to separate the supernatant fraction (s1) from the pellet. Samples of the s1 fraction (25 μ g total protein/well) were subjected to immunoblot analyses using a monoclonal antibody to myelin basic protein (MBP, 1:1000, clone SMI-99; Covance). Membranes were then re-probed with actin (1:1000, clone AC-40, Sigma-Aldrich), which served as a loading control. Protein expression was quantified using densitometry with the GeneSnap imaging system and software (SynGene, Frederick, MD). The integrated density values (IDV) of the 21.5-kDa and 18.5-kDa MBP bands were normalized to the IDV of the actin band.

Spatial learning and working memory assessment

Spatial learning in sham- and brain-injured mice was assessed using the Morris water maze as previously described (Huh et al., 2008). Each mouse was trained over 3 consecutive days (days 1–3 or days 4–6 post-injury), with 4 trials each day, and allotted a maximum of 60 sec to locate the eccentrically-placed submerged platform in a 1-m-diameter water maze. The average latency to reach the platform on each training day was computed as the average of 4 trials. At 24 h following the last set of trials, a transfer pipette was secured to the side of the platform and the latency to reach the platform was recorded in 2 trials (visible platform trial); the swim speed of the animal was also calculated. Working memory was assessed in the Morris water maze as previously described (Hoane et al., 2003), with the minor modification that the mice were released from a fixed starting point located on the periphery of the maze for all trials. The animals were required to locate the hidden platform using visual cues placed outside and around the pool. The platform was positioned in a different location on each of the 3 testing days. Each mouse was trained over 3 consecutive days (days 1–3 or days 7–9) with 4 trials each day, and allotted a maximum of 60 sec to locate the platform. The first trial of every day was deemed the “learning trial,” and the average of trials 2–4 was computed (Hoane et al., 2003).

Compound action potential measurements

CAPs in the corpus callosum were evaluated as previously described (Reeves et al., 2005). The mice were anesthetized

with isoflurane (5%), and decapitated, and the brains were quickly removed. Coronal slices (450 μ m) were cut on a Vibratome and placed in artificial cerebrospinal fluid (aCSF; pH 7.4), composed of (in mM): NaCl 130, KCl 3.5, $\text{Na}_2\text{H}_2\text{PO}_4$ 1.25, $\text{MgSO}_4 \cdot 7\text{H}_2\text{O}$ 1.5, $\text{CaCl}_2 \cdot 2\text{H}_2\text{O}$ 2, NaHCO_3 24, and glucose 10, and gassed with 95% O_2 /5% CO_2 . The sections were incubated for 1 h at room temperature and then transported to the recording chamber where they were submerged and perfused with aCSF (22°C) at a constant rate (3–4 mL/min) for the remainder of the experiment. Recordings were made at room temperature (22°C) in order to differentiate the myelinated (N1) and unmyelinated (N2) components of the CAPs (Reeves et al., 2005). A bipolar, tungsten stimulating electrode (inter-tip distance \sim 0.5 mm) was lowered into the corpus callosum about 0.5 mm lateral to the midline. A glass extracellular recording pipette (1–3 mega-ohm tip resistance when filled with aCSF) was lowered into the corpus callosum at approximately 1 mm from the stimulating electrode across the midline. Evoked CAPs were recorded using an Axoclamp 2b amplifier and digitized at 100 kHz. The amplitude of the CAPs was measured from standardized input–output curves from each slice, which were generated by increasing the intensity of stimulus pulses in 10 equal current steps (200 μ sec duration, 0.1 Hz), ranging from the threshold (the current where CAPs were first observed) to the maximum. To examine refractoriness, pairs of pulses were presented for which the inter-pulse interval increased in 0.5-msec steps from 3 msec to 12 msec using the maximum current level determined from the input–output curve for that slice.

Quantitative analysis was performed on waveforms that represented the average of 4 successive sweeps in each of 2 slices per animal. The difference from the first positive peak to the first trough was determined as the amplitude of the myelinated fibers (N1), while the difference between the second peak and the second trough was determined as the amplitude of the slower conducting unmyelinated fibers (N2). To analyze refractoriness of the N1 and N2 components, the CAP amplitude elicited by the second pulse (C2) in each paired stimulation was divided by the CAP amplitude elicited by the first pulse stimulation (C1), and this ratio was plotted as a function of the inter-pulse interval. The inter-pulse interval corresponding to the point at which the amplitude of the second pulse achieved 50% of that of the first pulse was determined.

Statistical analyses

All quantification was performed by an evaluator who was blinded to the injury status and survival time of the sample. All data are expressed as the mean \pm standard deviation. Comparisons of tissue water content, histologic data, immunoblot data, and acute neurologic parameters were determined using factorial one-way analysis of variance (ANOVA), followed by Newman-Keuls *post-hoc* testing if ANOVA rejected the null hypothesis. Spatial learning, working memory, and CAPs were analyzed using repeated-measures ANOVA, followed by Newman-Keuls *post-hoc* tests. Probe trial scores, swim speeds, and latencies to the visible platform were compared using Student's *t*-test for each time point. Refractoriness was compared using the Mann-Whitney *U* test. Only *p* values <0.05 were considered to be statistically significant.

Results

Acute neurological responses following closed head injury

Closed head injury in adult mice did not result in acute or delayed mortality. However, impact with the metal-tipped indenter resulted in a minor fracture perpendicular to the sagittal suture (arrow in Fig. 1C). Sham-injured mice righted themselves spontaneously within 15–20 sec after removal of anesthesia. In contrast, the return of the righting reflex (indicative of the duration of unconsciousness) was significantly longer after closed head injury (140–170 sec, $p < 0.05$, Table 1). Brain-injured mice experienced a brief period of apnea ranging from about 20–40 sec, which was not observed in sham-injured mice ($p < 0.05$, Table 1). Neither latency to the righting reflex nor the duration of apnea in the injured animals separated either by survival time post-injury within a study or across the multiple experiments was significantly different from each other, indicative of the consistency of the injury across the different groups.

Transient cognitive deficits following closed head injury

Closed head injury in the adult mouse resulted in spatial acquisition deficits in the Morris water maze when tested on days 1–3 post-injury (Fig. 2A). Although both sham- and brain-injured mice were able to locate the hidden platform over the 3-day testing period [day effect, ($F_{(2,26)}=4.1$, $p < 0.04$)], the time taken by brain-injured mice to reach the submerged platform was significantly greater compared to their sham-injured counterparts [injury effect, ($F_{(1,13)}=7.1$, $p < 0.025$)]. When a separate group of sham- and brain-injured mice was tested for spatial learning on days 4–6 post-injury, no deficit was observed [Fig. 2B, injury effect ($F_{(1,16)}=0.03$, $p = 0.86$)], and all animals learned the location of the platform over the 3 days of training [day effect, ($F_{(2,32)}=26.6$, $p < 0.001$)]. Closed head injury did not appear to cause motor impairment, based on the observation of similar swim speeds between sham-injured (21.0 ± 3.1 cm/sec) and brain-injured animals (20.3 ± 1.0 cm/sec). Visual impairment did not appear to be an issue in the brain-injured mice because the latency to the visible platform was not significantly different between sham-injured (11.1 ± 2.1 sec) and brain-injured mice (11.2 ± 2.4 sec). In addition to spatial learning deficits, brain-injured mice exhibited deficits in working memory in the acute (days 1–3) post-traumatic period, with an injury effect [Fig. 2C, ($F_{(1,13)}=6.6$, $p < 0.025$)], but not at a later time point (days 7–9) post-injury [Fig. 2D, ($F_{(1,13)}=2.5$, $p = 0.13$)].

Traumatic axonal injury following closed head injury

In sham-injured animals β -APP immunoreactivity was not observed in the corpus callosum (Fig. 3A). Closed head injury resulted in intra-axonal β -APP immunoreactivity that was observed as swellings in otherwise contiguous axons at 24 h post-injury (arrows in Fig. 3B), and predominantly as terminal bulbs at 3 days post-injury (arrowhead in Fig. 3C). Perisomatic axons containing β -APP were occasionally observed within the cortex below the impact site, and in the dorsomedial and dorsolateral thalamic nuclei (data not shown). In addition to the ventral hippocampal commissure and fimbria, swollen axonal profiles containing β -APP were observed along the central portion of the corpus callosum, extending

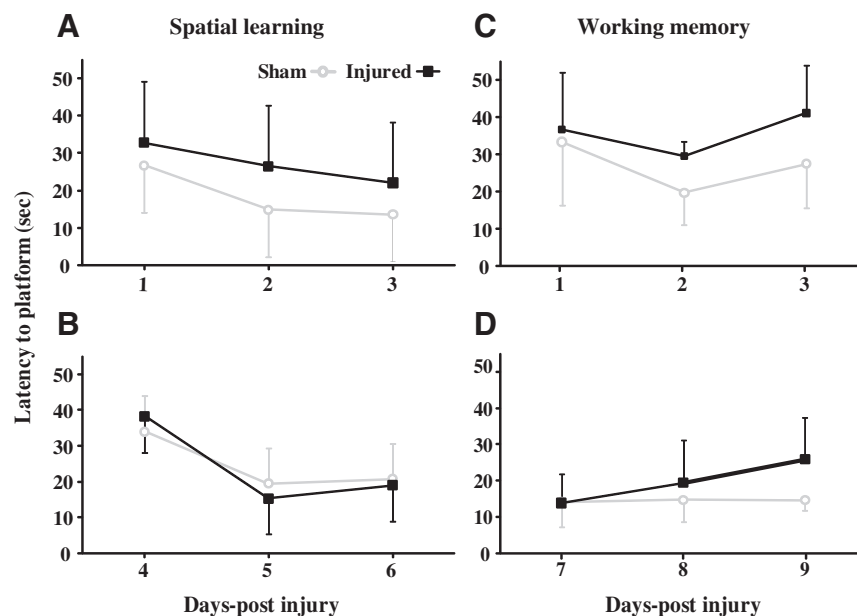


FIG. 2. Cognitive deficits following concussive brain trauma. Mice were tested for spatial learning (**A** and **B**), and working memory (**C** and **D**) abilities as described in the methods section. Repeated-measures analysis of analysis of variance (ANOVA) revealed an injury effect in both the spatial acquisition (**A**; $p < 0.025$) and the working memory (**C**; $p < 0.025$) paradigms on days 1–3 post-injury. No deficits were observed in spatial learning on days 4–6 post-injury (**B**), or in working memory on days 7–9 post-injury (**D**). All values are presented as mean \pm standard deviation.

away from the midline to white matter regions under the cingulum and in the lateral aspect of the white matter tract (top panel in Fig. 3J). By 3 days post-injury, the pattern of axonal β -APP staining was restricted to the fimbria and corpus callosum (middle panel in Fig. 3J). By 7 days, β -APP immunoreactivity was scarce (bottom panel in Fig. 3J), and by 14 days staining was absent (data not shown). Quantification of the extent of β -APP-reactive axonal profiles revealed an injury effect ($F_{(3,19)} = 63.4$, $p < 0.0001$, Fig. 3K). *Post-hoc* analysis indicated that there were significantly more injured axonal profiles at 24 h ($p < 0.001$) and 3 days post-injury ($p < 0.01$) compared to sham-injured animals, greater axonal injury at 24 h than at 3 ($p < 0.001$) or 7 days ($p < 0.001$), and at 3 days compared to 7 days ($p < 0.001$). At 7 days post-injury, the extent of axonal β -APP reactivity was not significantly different from that in sham-injured animals (Fig. 3K).

Axonal synaptophysin (SYP) immunoreactivity was used to specifically evaluate transport impairment in the anterograde direction. In brains from sham-injured mice, immunoreactivity for SYP demonstrated a diffuse granular pattern in the cortex (data not shown), and was absent in underlying white matter (Fig. 3D). Following closed head injury, SYP staining was evident in axons and appeared as swellings in a linear pattern along the length of the axon at 24 h (arrows in Fig. 3E), and as larger diameter swellings at 3 days following injury (arrowhead in Fig. 3F). Few if any SYP-positive axonal profiles were present at 7 days following injury (data not shown). Axonal immunoreactivity for SYP was only observed in the corpus callosum below the site of impact (Fig. 3J).

The presence of dephosphorylated neurofilaments within axons (Christman et al., 1994), detected using the SMI-32 antibody, has been used as an indicator of TAI. Compared to sham-injured brains (Fig. 3G), intra-axonal SMI-32 immunoreactivity was observed at 24 h post-injury (Fig. 3H and I),

either as increased varicosity (arrows in Fig. 3H), or as terminal bulbs (arrowhead in Fig. 3H). At 3 (arrowhead in Fig. 3I) and 7 days post-injury, the extent of SMI-32-positive axonal swellings was reduced.

Axonal degeneration following closed head injury

Fluoro-Jade-B histochemistry was used to determine if TAI was associated with axonal degeneration (Schmued et al., 1997). In sham-injured animals (Fig. 4A), and at 24 h following closed head injury (Fig. 4B), there was no evidence of Fluoro-Jade-B-positive axonal profiles within any white matter tract analyzed. At 7 (data not shown) and 14 days post-injury (Fig. 4C), Fluoro-Jade-B staining was evident in the corpus callosum as swollen axonal segments (arrow in Fig. 4C), and terminal bulbs (arrowhead in Fig. 4C), and in the cingulum and lateral white matter tracts. These observations suggest that axons continue to degenerate after accumulation of APP, synaptophysin or dephosphorylated neurofilament are no longer visible. Despite the presence of TAI and axonal degeneration, Nissl-cyanine R histochemistry did not reveal overt differences in the corpus callosum (Fig. 4D and E), cingulum, and lateral white matter tracts (data not shown) between sham- and brain-injured animals. Immunoblot analysis did not show any differences in the expression of MBP in white matter tracts between sham-injured and brain-injured animals at any time point post-injury, for either the 21.5-kDa ($F_{(3,12)} = 2.8$, $p = 0.09$) or 18.5-kDa band ($F_{(3,12)} = 1.3$, $p = 0.32$, Fig. 4F).

Retrograde axonal transport deficits following closed head injury

The presence of acute TAI and chronic axonal degeneration led us to evaluate the integrity of retrograde axonal transport using Fluoro-Gold (FG). Confirmation that FG transport oc-

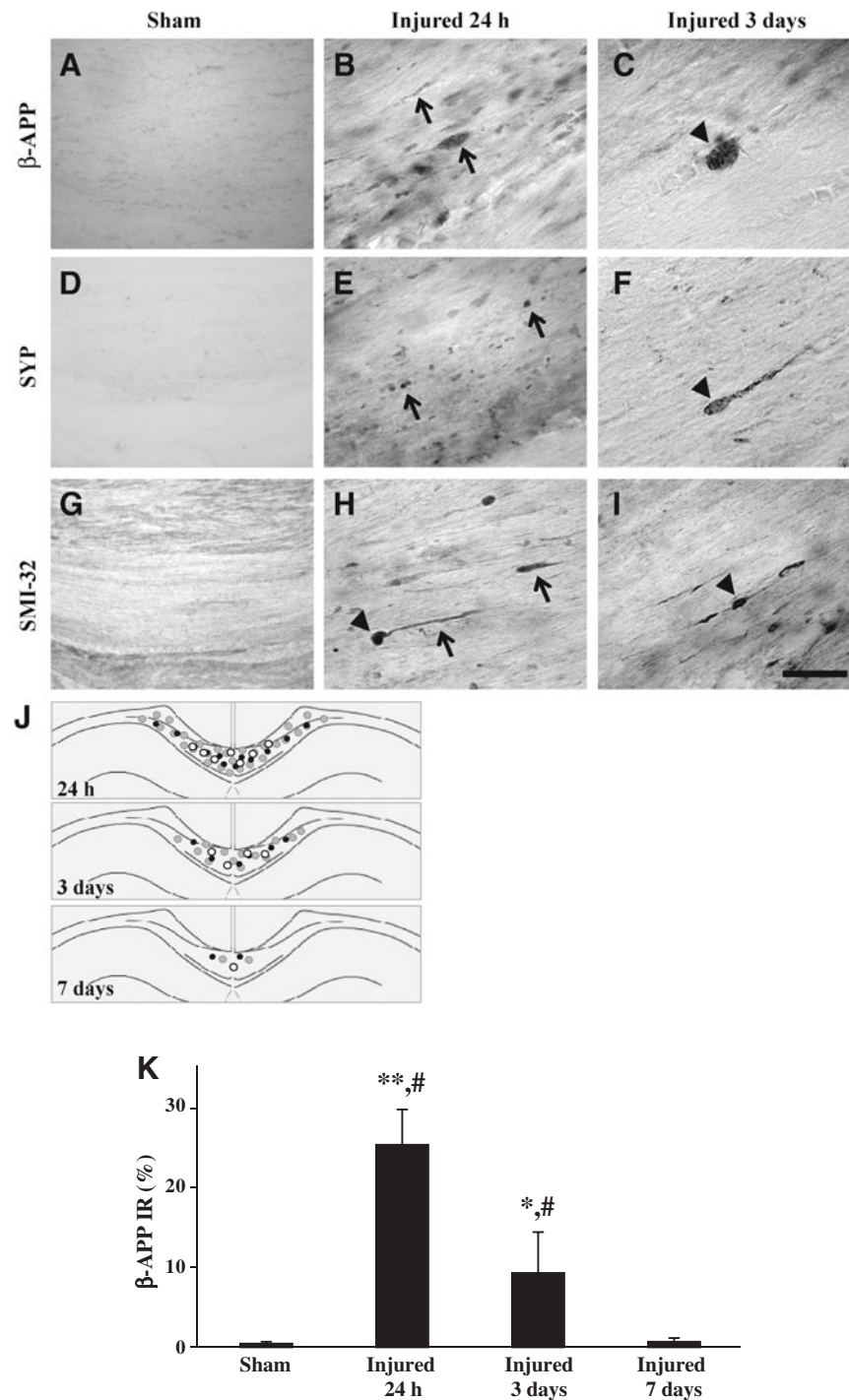


FIG. 3. Traumatic axonal injury following concussive brain trauma. Representative photomicrographs demonstrating intra-axonal immunoreactivity for β -amyloid precursor protein (β -APP, A–C), synaptophysin (SYP, D–F), and dephosphorylated neurofilament (SMI-32, G–I), in the corpus callosum at 24 h (B, E, and H), and 3 days (C, F, and I) following impact. Note the absence of immunoreactivity for all three proteins in sham-injured brains (A, D, and G). β -APP-positive profiles were identified as swellings along contiguous axons (arrows in B), and terminal bulbs (arrowhead in C). SYP immunoreactivity was present as punctate staining (arrows in E), and larger swellings (arrowhead in F). SMI-32-positive profiles were apparent as swellings (arrows in H), and retraction balls (arrowheads in H and I). (J) Schematic diagram showing the spatial distribution of β -APP (gray circles), SYP (white circles), and SMI-32 (black circles), at 24 h (top panel), 3 days (middle panel), and 7 days (bottom panel) post-injury. (K) Quantification of the extent of intra-axonal β -APP immunoreactivity in white matter tracts below the site of impact. All values are presented as mean \pm standard deviation (* p < 0.01, ** p < 0.001 compared to sham-injured brains; # p < 0.001 compared to 3 or 7 days post-injury; scale bar = 100 μ m for panels A, D, and G, and 20 μ m for all other panels).

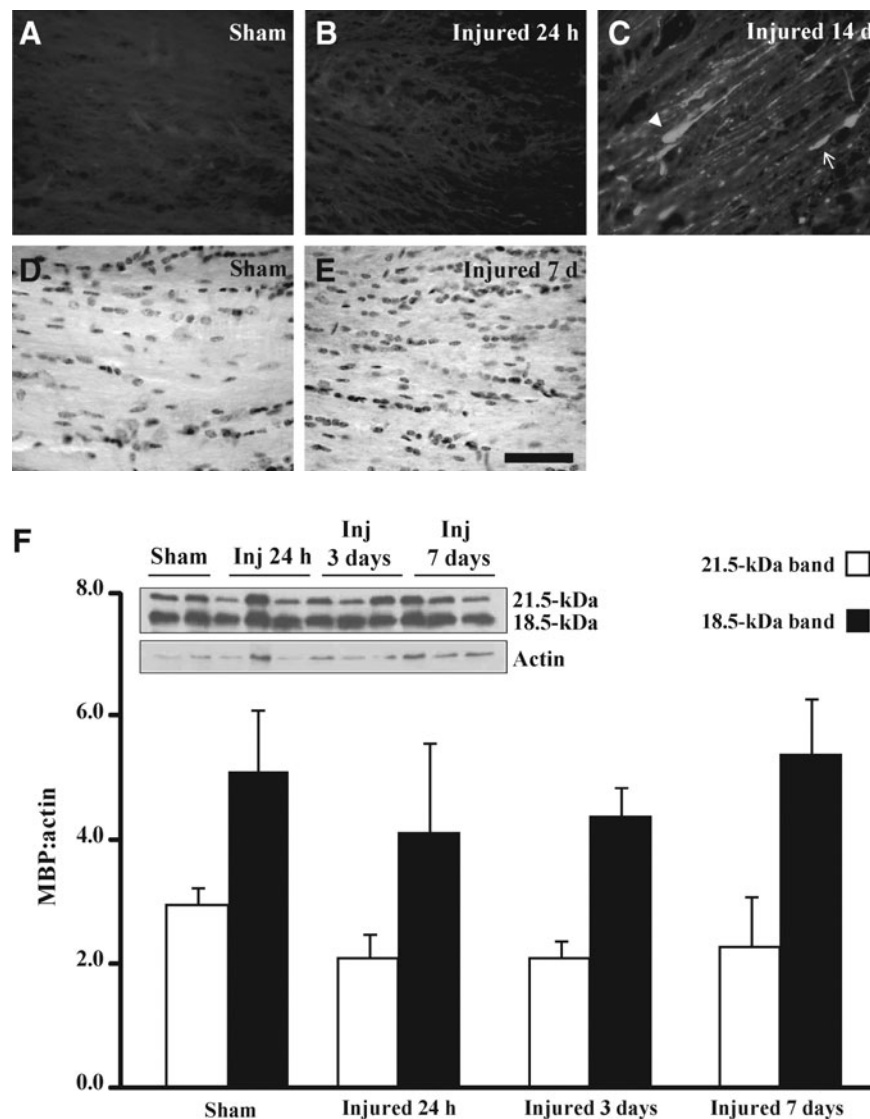


FIG. 4. Axonal degeneration following concussive brain trauma. Representative photomicrographs demonstrating Fluoro-Jade B-reactive axons in the corpus callosum at 14 days post-injury (C), but not in either sham-injured animals (A), or at 24 h following injury (B). Note the appearance of swollen axonal segments (arrow in C), and terminal bulbs (arrowhead in C). Panels D (sham-injured) and E (7 days post-injury) are photomicrographs of Nissl-cyanine R staining in the corpus callosum. (F) Representative immunoblots of myelin basic protein from lysates of corpus callosum of sham-injured animals, and at 24 hours (Inj 24 h), 3 days (Inj 3 days), and 7 days (Inj 7 days) post-injury, demonstrating the characteristic 21.5- and 18.5-kDa bands. Quantification of optical density as a function of actin (loading control) is presented in the graph. All values are presented as mean \pm standard deviation (scale bar = 20 μ m for panels A–C, and 50 μ m for panels D and E).

current via callosal fibers was based on the observation that transection of the corpus callosum led to a complete absence of FG-positive cells in the homotypic cortex contralateral to the injection site (Fig. 5B). Furthermore, intense FG staining at the site of injection (Fig. 5A) to similar extents in sham-injured and brain-injured animals suggested that closed head injury did not affect uptake of FG at axon terminals. At 2 days after the injection of FG into the cortex of sham-injured animals, FG-positive cell bodies were detected in the homotypic cortex contralateral to the injection site (Fig. 5C). Higher magnification revealed the canonical particulate nature of FG within cell bodies (inset in Fig. 5C). In contrast, when FG was injected at 12 days following closed head injury and the animals were sacrificed 48 h later, there was a noticeable reduction in the

extent of FG-labeled cells in the cortex contralateral to the injection site (Fig. 5D). Quantitative analysis revealed that this reduction was present as early as 24 h post-injury, and was sustained until 12 days [Fig. 5E, ($F_{(3,24)} = 3.1$, $p < 0.05$ by one-way ANOVA)]. *Post-hoc* analysis indicated that the number of FG-positive cells in the sham-injured brains was significantly greater than at 1 ($p < 0.04$), 5 ($p < 0.025$), and 14 days ($p < 0.025$, Fig. 5E) post-injury.

Compound action potentials following closed head injury

Evoked CAPs were used to determine whether structural and functional alterations in the white matter were associated

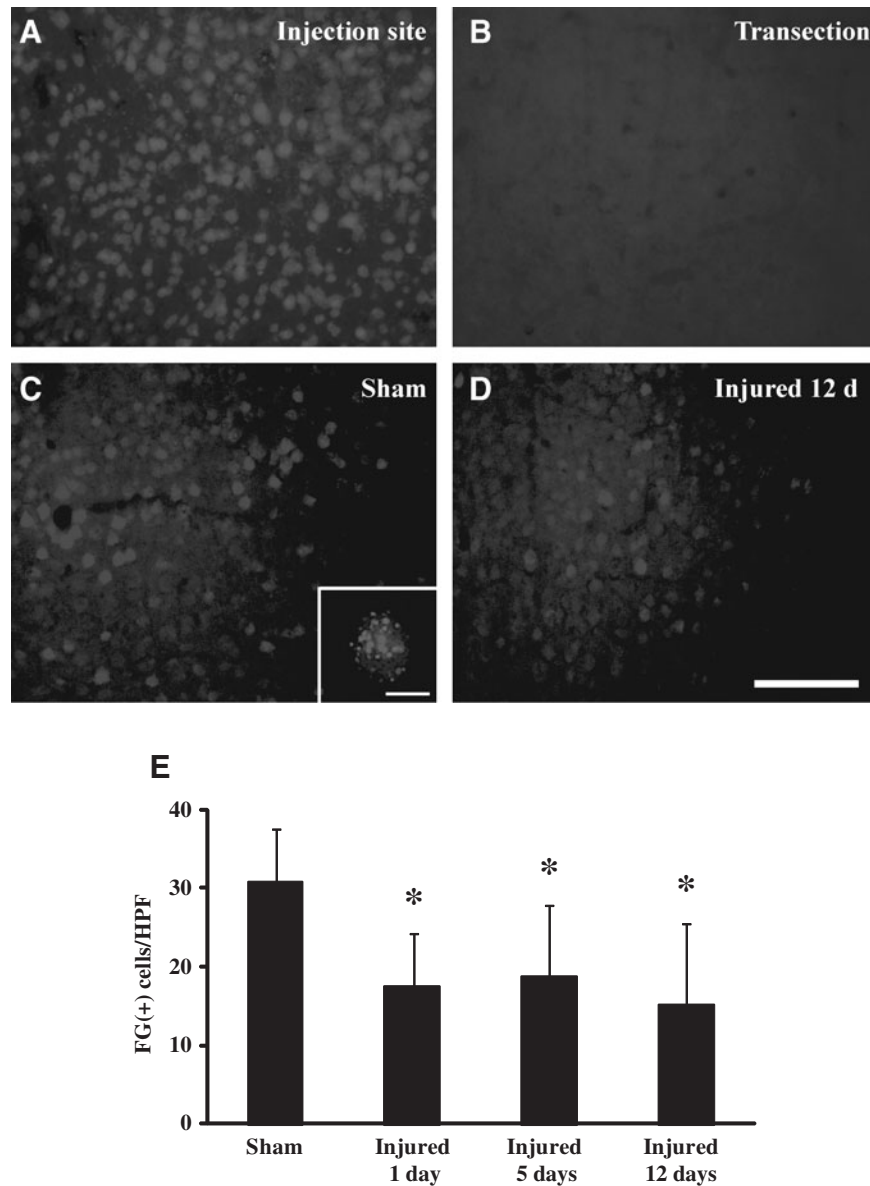


FIG. 5. Impaired retrograde transport following concussive brain trauma. Representative photomicrographs demonstrating Fluoro-Gold (FG)-labeled cell bodies in the cortex. (A) FG-positive cell bodies at the site of injection in sham-injured mice. (B) Note the absence of FG-labeled cell bodies in the cortex contralateral to the site of injection following transection of callosal fibers. (C) FG-positive cell bodies in the homotypic cortex contralateral to the site of injection in sham-injured mice. (D) At 14 days post-injury; note the particulate nature of FG (see also inset in C). (E) Quantification of FG-positive cells was performed as described in the methods section. All values are presented as mean \pm standard deviation (HPF, high-powered field; * $p < 0.05$ compared to sham-injured animals; scale bar = 100 μ m for panels A–D, and 10 μ m for inset in panel C).

with axonal conduction deficits. As observed in adult rats (Reeves et al., 2005), evoked CAPs in adult sham-injured and brain-injured mice resulted in a biphasic waveform comprised of an initial segment (N1), representing the fast-conducting myelinated axons, followed by a second component of the waveform (N2), which characterized the slower-conducting unmyelinated axons (Fig. 6A). Quantitative analysis of CAPs recorded from injured slices revealed a decrease in amplitude for the N1 component [injury effect, ($F_{(1,18)} = 16.6$, $p < 0.001$ Fig. 6B)], which was independent of survival time [injury \times time effect, ($F_{(1,18)} = 0.02$, $p = 0.90$, Fig. 6B)]. The amplitude for the N2 component did not show a

difference between the sham-injured and brain-injured groups at any time point post-injury [injury effect, ($F_{(1,16)} = 0.4$, $p = 0.56$, Fig. 6C)]. Refractoriness, indicative of the time required to depolarize the membrane from a hyperpolarized state into a range in which a second action potential can be initiated, for the myelinated (N1) fibers did not differ between the sham and injured groups at both 24 h ($p = 0.70$), and 14 days ($p = 0.12$, Fig. 6D). For the unmyelinated (N2) fibers, the refractoriness was no different between slices from sham-injured and brain-injured mice at 24 h ($p = 0.70$); however, at 14 days post-injury, the amount of time required for refractoriness to reach 50% was significantly longer in slices from

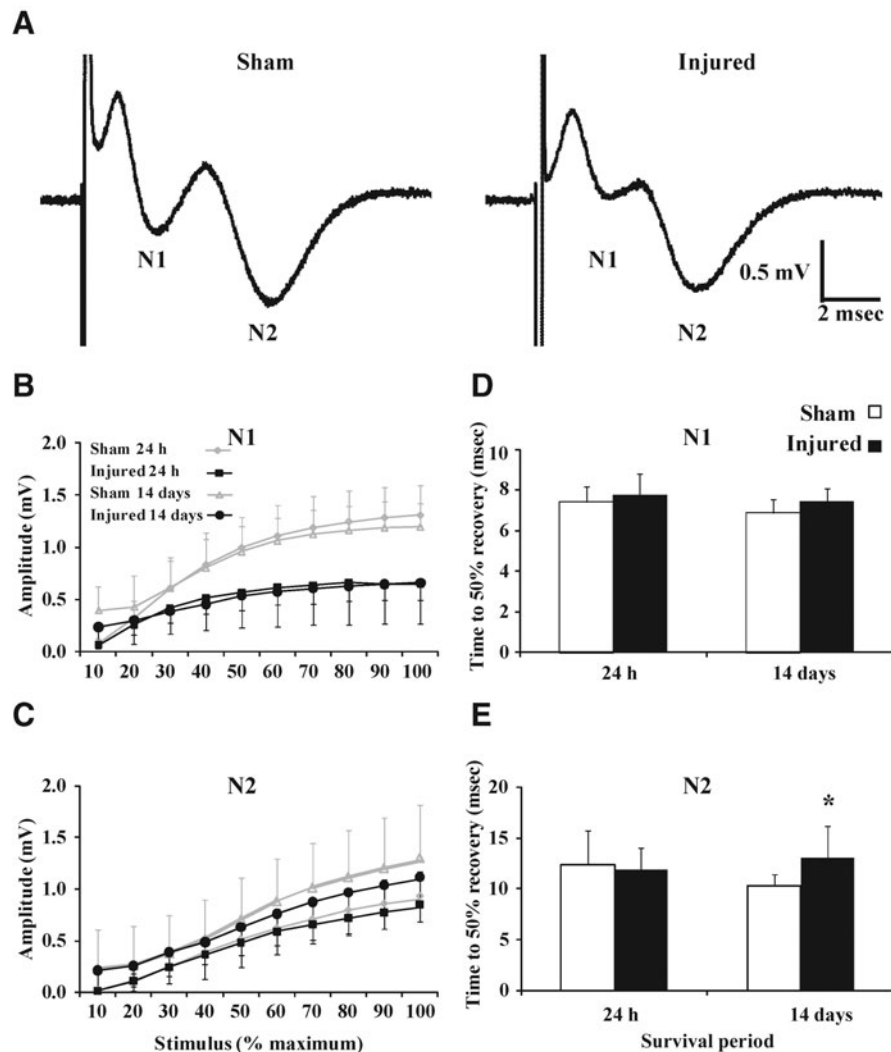


FIG. 6. Inhibition of compound action potentials (CAPs) of myelinated fibers following concussive brain trauma. (A) Representative traces of evoked CAPs in sham- and brain-injured mice at 24 h post-injury. Evoked CAPs of (B) myelinated (N1) and (C) unmyelinated (N2) axons in the corpus callosum were measured as described in the methods section. Repeated-measures analysis of variance of CAP amplitude revealed an injury effect for the myelinated ($p < 0.001$), but not the unmyelinated, component. Refractoriness for the (D) myelinated and (E) unmyelinated fibers at 24 h and 14 days post-injury ($*p < 0.04$). All values are presented as mean \pm standard deviation.

injured brains than in those from sham-injured brains ($p < 0.04$, Fig. 6E). The conduction velocity of either the N1 or the N2 component was not affected by injury at either survival time point (data not shown).

Cortical damage following closed head injury

In sham-injured animals, there was no evidence of Fluoro-Jade-B reactivity in any region of the cortex (Fig. 7A). At 24 h following CBI, degenerating neurons were observed along the granular and agranular retrosplenial cortex in both hemispheres (Fig. 7B). The pattern of Fluoro-Jade-B-positive cells often extended laterally along the cortex corresponding to the primary and supplementary motor cortex, the lateral parietal cortex, and the trunk region of the primary sensory cortex. Quantitative analysis of Fluoro-Jade-B-positive cells in the cortex revealed an injury effect ($F_{(3,20)} = 26.8$, $p < 0.0001$);

post-hoc analysis demonstrated significantly more Fluoro-Jade-B-positive cells at 24 h compared to sham-injured animals ($p < 0.001$), and at 3 ($p < 0.001$) and 7 days ($p < 0.001$) following injury (Fig. 7C). In addition, there was a greater extent of cortical Fluoro-Jade-B staining at 3 days post injury compared to sham-injured animals ($p < 0.03$). Nissl staining of adjacent sections revealed shrunken and intensely-stained cells at 24 h (Fig. 7E) and 7 days post-injury (Fig. 7F), compared to similar regions in the sham-injured animals (Fig. 7D). Although impact with the metal-tipped indenter fractured the skull, hemorrhagic tissue tears were not observed in the cortex of the majority of injured animals; however, hemorrhage in the cortex immediately below the impact site was present in 2/6 animals from at 24-h survival time point (data not shown). Despite the lack of intracerebral hemorrhage, closed head injury in the mouse resulted in a significant increase in the tissue water content, reflective of edema, in the cortex

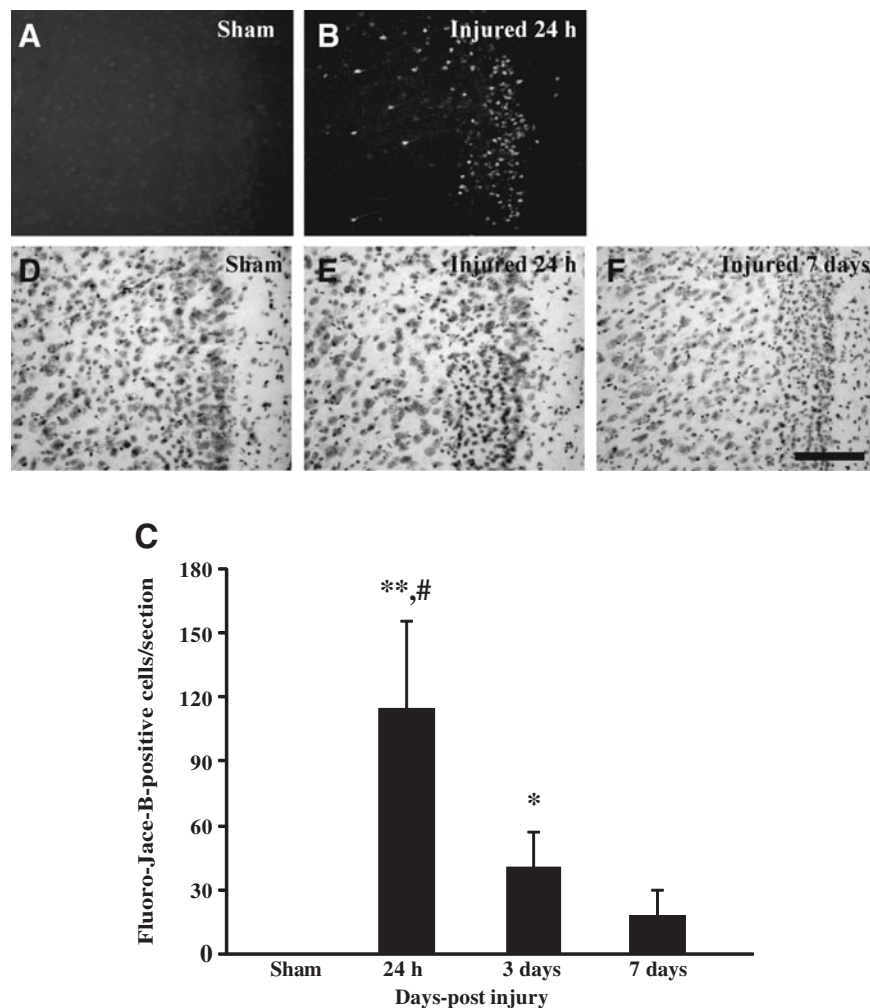


FIG. 7. Neurodegeneration in the cortex following concussive brain trauma. Representative photomicrographs illustrating Fluoro-Jade-B reactivity in the retrosplenial cortex in (A) sham-injured animals, and (B) at 24 h post-injury. (C) Quantification of the number of Fluoro-Jade-B-positive cells in the cortex below the site of impact. All values are presented as mean \pm standard deviation (* $p < 0.05$, ** $p < 0.001$ compared to sham-injured brains; # $p < 0.001$ compared to 3 or 7 days post-injury). Panels D–F are photomicrographs of Nissl staining in the retrosplenial cortex of (D) sham-injured brains, and at (E) 24 h, and (F) 7 days post-injury. Note the increased cellularity in the brain-injured animals (scale bar = 100 μ m for all panels).

compared to sham-injured animals over the first 24 h post-surgery/injury [injury effect, ($F_{(1,25)} = 4.6$, $p < 0.04$; no time effect, Fig. 8)]. Similar analysis in the hippocampus and thalamus did not reveal increases in tissue water content at any time post-injury (Fig. 8).

Neurodegeneration in the hippocampus following closed head injury

Overt loss of neurons in either the pyramidal layer (data not shown), or the granule layer of the dentate gyrus (Fig. 9A and B), was not apparent up to 7 days following CBI. At 24 h, patches of intensely-stained, non-neuronal cells were observed in the granule cell layer (Fig. 9A). Fluoro-Jade-B-positive cells predominated in the hilus of the dentate gyrus at 24 h (Fig. 9C), and were additionally observed in the granule cell layer of the dentate gyrus at 3 days (data not shown); little to no evidence of neurodegeneration was present at 7 days post-injury (Fig. 9D). Quantitative analysis of Fluoro-Jade-B-

positive cells in the dentate gyrus revealed an injury effect ($F_{(3,20)} = 10.5$, $p < 0.001$). *Post-hoc* analysis demonstrated that there were significantly more Fluoro-Jade-B-positive cells at 24 h compared to sham-injured animals ($p < 0.001$), at 3 ($p < 0.01$) and 7 days ($p < 0.001$) following injury (Fig. 9E). Immunoreactivity for synaptophysin was assessed between 24 h and 14 days post-injury as a measure of synaptic alterations in the hippocampus (Fig. 9F–H). The classic trilaminar pattern of synaptophysin immunoreactivity in the molecular layer of the dentate gyrus was present in both sham-injured (Fig. 9F) and brain-injured animals at 24 h (Fig. 9G), 3 days (data not shown), 7 days (data not shown), and 14 days (Fig. 9H) post-injury, indicating that no overt loss of synapses accompanied CBI in the mouse.

Discussion

This report describes a model of concussion that is characterized by a brief loss of consciousness and deficits in spatial

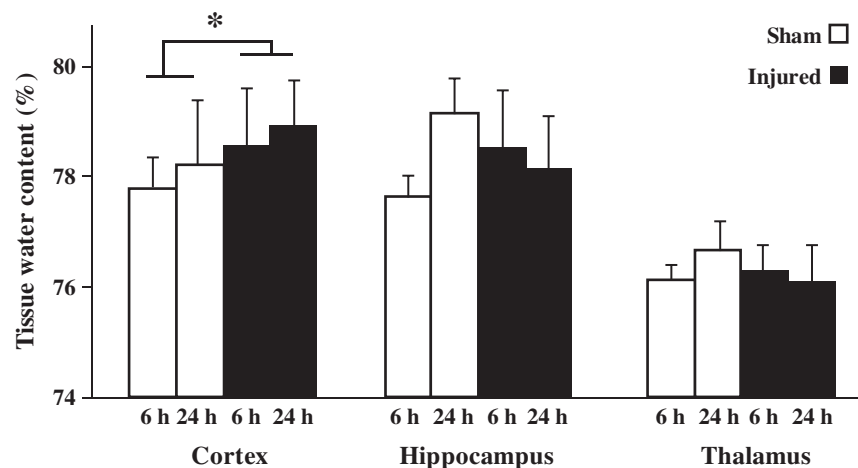


FIG. 8. Brain edema following concussive brain trauma. Tissue water content was measured in the cortex, hippocampus, and thalamus as described in the methods section. Factorial analysis of variance revealed that brain trauma significantly increased edema in the underlying cortex compared to sham-injured animals over the first 24 h post-surgery/injury. All values are presented as mean \pm standard deviation (* $p < 0.05$ compared to sham-injured brains).

learning and working memory over the first 3 days post-injury. The cognitive deficits were accompanied by increased tissue water content in the cortex, diffuse neurodegeneration in the retrosplenial cortex and the hilus of the dentate gyrus, and TAI in the corpus callosum and cingulum, leading to axonal degeneration. Direct evidence of functional damage to axons was provided by decreased retrograde transport and lowered amplitude of CAPs of myelinated axons. Importantly, edema, neurodegeneration, TAI, and cognitive deficits were only observed in the acute (1–3 days) post-traumatic period, whereas axonal degeneration and deficits in retrograde transport and axonal conductance were evident up to 2 weeks post-injury, suggesting that the concussed brain continues to demonstrate evidence of cellular dysfunction despite resolution of behavioral deficits.

Cognitive deficits have been observed in existing models of concussive brain trauma in both rats and mice (Hamm et al., 1996; Lyeth et al., 1990; Spain et al., 2010; Tang et al., 1997a; Zohar et al., 2003). Brain injury as a result of impact to the intact skull of mice resulted in spatial learning deficits (Zohar et al., 2003), and in latent learning deficits at 1 and 2 weeks using a water-finding task (Tang et al., 1997a). Fluid-percussion trauma resulted in spatial learning deficits from 1 week up to 3 months following injury in mice (Spain et al., 2010) and rats (Lyeth et al., 1990), and working memory deficits up to 2 weeks post-injury in rats (Hamm et al., 1996). In the present study, impairments in spatial learning and working memory were observed only in the first 3 days post-injury, validating the transient nature of post-concussive cognitive deficits; concussed patients suffer acute memory loss and difficulty maintaining attention, which resolve within 2 weeks following injury (McCrory et al., 2009). While differences in mouse strain may explain some of these discrepancies in cognitive findings, it is unlikely that the transient nature of our deficits can be explained by a lesser degree of injury severity, since the range of righting reflex latency was similar to that reported in previous studies (Longhi et al., 2005; Spain et al., 2010; Tang et al., 1997a). Interestingly, Longhi and colleagues reported that unilateral impact on the intact skull did not produce any spatial learning

deficits over the first 3 days (Longhi et al., 2005), suggestive of the importance of the location of the impact in producing diffuse brain damage.

Traumatic axonal injury (TAI) is a hallmark of diffuse TBI, including concussion (Blumbers et al., 1994; Oppenheimer, 1968). Importantly, a strong correlation between TAI, as indicated by decreased fractional anisotropy in white matter tracts, and cognitive dysfunction has been demonstrated in humans (Kraus et al., 2007; Kumar et al., 2009; Wozniak et al., 2007). Intra-axonal APP accumulation is recognized as a marker of TAI and indicates impaired axonal transport (IAT; Buki and Povlishock, 2006), although the link between APP accumulation and behavioral deficits is not clearly understood. Spain and colleagues suggest that intra-axonal APP accumulation may represent the cellular basis for impaired spatial learning following TBI (Spain et al., 2010). However, spatial learning deficits were not observed following concussive TBI, despite the presence of APP accumulations within axons (Longhi et al., 2005), while Tweedie and colleagues failed to observe intra-axonal APP accumulation in animals that exhibited depressive behavior following TBI (Tweedie et al., 2007). Because APP can be transported in both anterograde (Buxbaum et al., 1998; Koo et al., 1990) and retrograde (Papp et al., 2002) directions, we provide additional evidence that transport in either direction is impaired. Thus the presence of SYP, a component of synaptic vesicles (Wiedenmann and Franke, 1985), in axonal swellings strongly implies IAT in the anterograde direction, an observation similar to that seen following brain injury in the rat (Shoji and Kibayashi, 2006). In addition, we demonstrate for the first time evidence of retrograde transport impairment in the brain following a traumatic injury, which validates an earlier report of reduced Fluoro-Gold transport to the retinal ganglion cell layer from the superior colliculus following optic nerve stretch injury (Saatman et al., 2003). The cellular mechanisms underlying IAT have yet to be described and may be mediated by alterations in axonal structure (Buki and Povlishock, 2006). In this regard, neurofilament compaction, which occurs as a result of dephosphorylation, may lead to IAT, and has

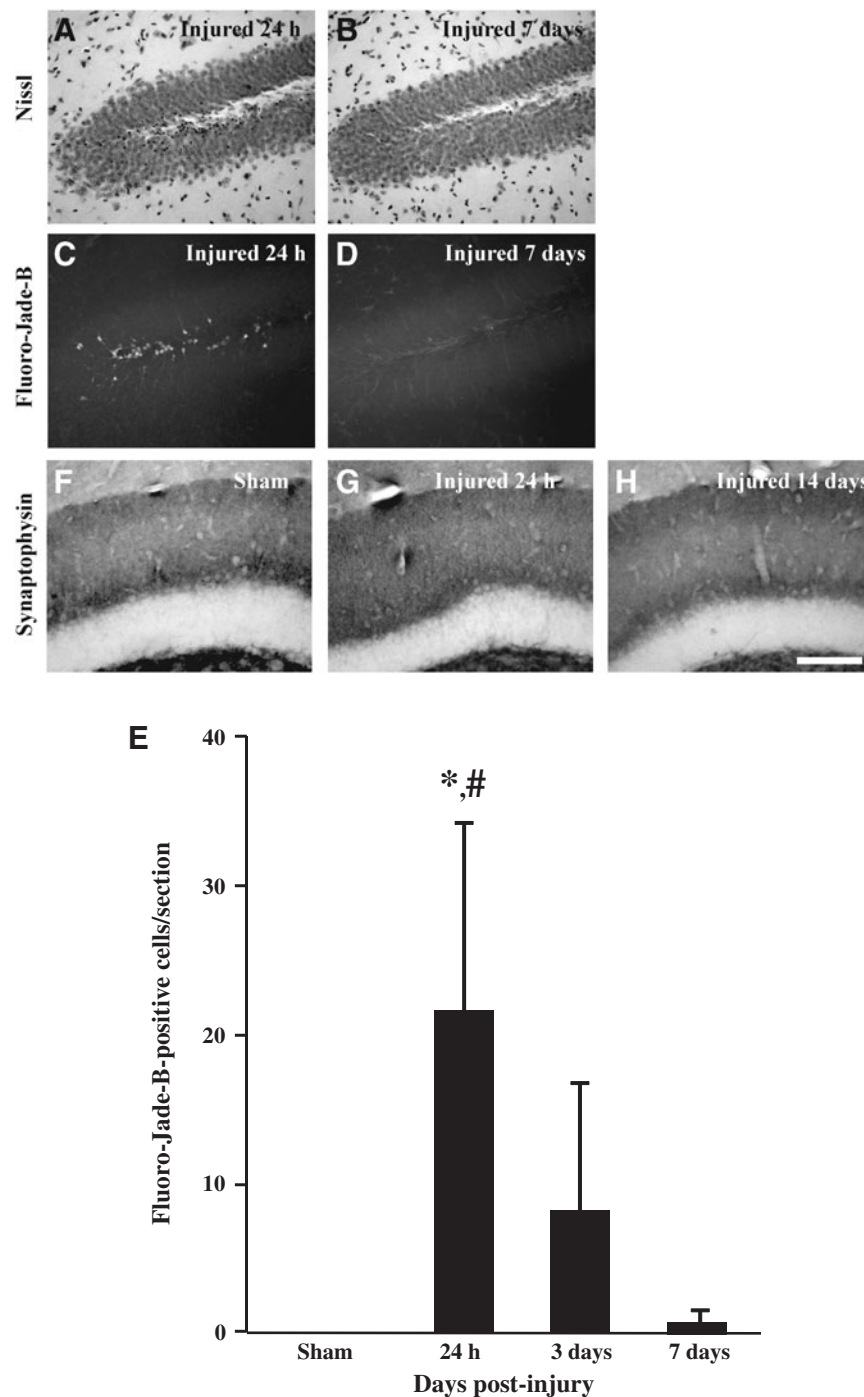


FIG. 9. Neurodegeneration and synaptophysin immunoreactivity in the hippocampus following concussive brain trauma. Shown are representative photomicrographs of Nissl-stained sections, demonstrating a lack of change in the cellularity in the granule cell layers of the dentate gyrus at 24 h (A) and 7 days (B) post-injury. Fluoro-Jade-B-positive cells were present in the hilus of the dentate gyrus at 24 h (C), but not at 7 days (D) post-injury. (E) Quantification of Fluoro-Jade-B-positive cells was performed as described in the methods section. All values are presented as mean \pm standard deviation (* $p < 0.001$ compared to sham animals; # $p < 0.01$ compared to 3 or 7 days post-injury). Synaptophysin immunoreactivity was visualized as the classic trilaminar pattern of dark-light-dark staining in the molecular layer of the dentate gyrus in both sham-injured (F) and brain-injured animals at 24 h (G) and 14 days (H) post-injury (scale bar = 100 μ m for all panels).

been recognized as another prominent characteristic of TAI following TBI (Chen et al., 1999; Christman et al., 1994; Povlishock et al., 1997). Although co-localization experiments were not performed in the present study, axons containing dephosphorylated neurofilament were observed in regions where axons containing accumulated APP or SYP were present, suggestive of an association between transport impairment and cytoskeletal alterations. It must be noted that in certain tracts of the traumatically-injured rat brain, co-localization of accumulated APP and compacted neurofilament has not been observed (DiLeonardi et al., 2009; Marmarou et al., 2005).

Impaired axonal transport was accompanied by decreased axonal conductance within the corpus callosum, confirming the results of earlier studies of diffuse TBI in adult rats, in which reductions in the amplitude of compound action potentials in both myelinated (Baker et al., 2002; Reeves et al., 2005) and unmyelinated axons were observed (Reeves et al., 2005). However, unlike in previous reports (Baker et al., 2002; Reeves et al., 2005), we did not observe any recovery of CAP amplitude up to 14 days post-injury. While it may be possible that there is no causal link between axonal conduction and cognitive deficits, the discrepancy between this sustained reduction in CAP amplitude and the transient cognitive deficits may also reflect the differential sensitivity of the two outcome measures. The reduction in CAP amplitude in our studies was restricted to myelinated axons, whereas in the brain-injured adult rat, the unmyelinated axons were more susceptible (Reeves et al., 2005). In part, the differences between our observations and those published previously may be attributed to species and injury model differences, and was less likely a function of injury severity, since the righting reflex latencies in the rat were greater than those observed in the mouse (Reeves et al., 2005). We suggest that the sustained deficits observed in the present study may reflect axonal degeneration detected using Fluoro-Jade-B histochemistry (Goda et al., 2002; Hallam et al., 2004; Huh et al., 2008; Ohlsson et al., 2004; Schmued et al., 1997; Shoji and Kibayashi, 2006; Tong et al., 2002). It must be noted that the immunohistochemical markers of TAI (APP, SYP, and dephosphorylated neurofilament) were not as apparent after the first 3 days post-injury, suggesting that evaluation of damage in the chronic period may require additional indicators of axonal injury.

It has been suggested that neurodegeneration in the cortex and hippocampus may be one mechanism underlying the post-traumatic behavioral deficits (Longhi et al., 2005; Spain et al., 2010; Tang et al., 1997b; Tashlykov et al., 2007). The presence of Fluoro-Jade-B-positive neurons in the hilus may explain the transient spatial learning deficits (Hicks et al., 1993; Tang et al., 1997a), although we did not find evidence of neurodegeneration in areas CA2 and CA3 of the hippocampus, in contrast to a previous study (Tang et al., 1997b). It is important to note that hippocampal cell death is not always associated with learning deficits, as suggested by the observations seen following diffuse TBI in the rat (Miyazaki et al., 1992; Reeves et al., 1997). While it is not certain if there are deficits in long-term potentiation in brain-injured mice, we did not observe overt alterations in SYP immunoreactivity in the dentate gyrus, as has been reported in the rat (Phillips et al., 1994). Diffuse neurodegeneration in the retrosplenial cortex, possibly due to the observed edema (Longhi et al., 2005; Tang et al., 1997b; Zohar et al., 2003), may explain the

deficits in working memory. Animals with lesions of the retrosplenial cortex make more errors in the eight-arm radial arm maze task of working memory compared to controls (Keene and Bucci, 2009; Pothuizen et al., 2010). It must be noted that neither overt neuronal loss nor caspase activation (data not shown) was observed, despite the presence of both Fluoro-Jade-B staining and morphologic changes, suggesting that neuronal dysfunction, rather than neuronal loss, may underlie the behavioral deficits seen.

In summary, we have developed a clinically-relevant model of concussive brain injury in the adult mouse that exhibits acute cognitive deficits accompanied by axonal injury. However, despite the transient nature of the cognitive deficits, reduced transport and conduction in axons, along with evidence of axonal degeneration, suggest that the concussed brain continues to demonstrate evidence of cellular dysfunction and damage. This model allows the development of strategies to evaluate the mechanisms underlying axonal damage uncomplicated by an accompanying contusion, with a view toward developing treatment strategies that are targeted to the concussed patient.

Acknowledgments

We would like acknowledge the efforts of Ms. Rachel Tang for the analysis of the electrophysiology data. These studies were supported in part by grants from the NIH (no. HD41699 and NS065017 to R.R.), and a VA Merit Review grant to R.R. and A.T.

Author Disclosure Statement

No competing financial interests exist.

References

- Arfanakis, K., Haughton, V.M., Carew, J.D., Rogers, B.P., Dempsey, R.J., and Meyerand, M.E. (2002). Diffusion tensor MR imaging in diffuse axonal injury. *AJNR Am. J. Neuroradiol.* 23, 794–802.
- Baker, A.J., Phan, N., Moulton, R.J., Fehlings, M.G., Yucel, Y., Zhao, M., Liu, E., and Tian, G.F. (2002). Attenuation of the electrophysiological function of the corpus callosum after fluid percussion injury in the rat. *J. Neurotrauma* 19, 587–599.
- Bazarian, J.J., McClung, J., Shah, M.N., Cheng, Y.T., Flesher, W., and Kraus, J. (2005). Mild traumatic brain injury in the United States, 1998–2000. *Brain Inj.* 19, 85–91.
- Blumbers, P.C., Scott, G., Manavis, J., Wainwright, H., Simpson, D.A., and McLean, A.J. (1994). Staining of amyloid precursor protein to study axonal damage in mild head injury. *Lancet* 344, 1055–1056.
- Buki, A., and Povlishock, J.T. (2006). All roads lead to disconnection?—Traumatic axonal injury revisited. *Acta Neurochir. (Wien.)* 148, 181–193; discussion 193–194.
- Buxbaum, J.D., Thinakaran, G., Koliatsos, V., O'Callahan, J., Slunt, H.H., Price, D.L., and Sisodia, S.S. (1998). Alzheimer amyloid protein precursor in the rat hippocampus: transport and processing through the perforant path. *J. Neurosci.* 18, 9629–9637.
- Chen, X.H., Meaney, D.F., Xu, B.N., Nonaka, M., McIntosh, T.K., Wolf, J.A., Saatman, K.E., and Smith, D.H. (1999). Evolution of neurofilament subtype accumulation in axons following diffuse brain injury in the pig. *J. Neuropathol. Exp. Neurol.* 58, 588–596.

- Christman, C.W., Grady, M.S., Walker, S.A., Holloway, K.L., and Povlishock, J.T. (1994). Ultrastructural studies of diffuse axonal injury in humans. *J. Neurotrauma* 11, 173–186.
- Dempsey, R.J., Baskaya, M.K., and Dogan, A. (2000). Attenuation of brain edema, blood-brain barrier breakdown, and injury volume by ifenprodil, a polyamine-site N-methyl-D-aspartate receptor antagonist, after experimental traumatic brain injury in rats. *Neurosurgery* 47, 399–404; discussion 404–406.
- DiLeonardi, A.M., Huh, J.W., and Raghupathi, R. (2009). Impaired axonal transport and neurofilament compaction occur in separate populations of injured axons following diffuse brain injury in the immature rat. *Brain Res.* 1263, 174–182.
- Dixon, C.E., Lyeth, B.G., Povlishock, J.T., Findling, R.L., Hamm, R.J., Marmarou, A., Young, H.F., and Hayes, R.L. (1987). A fluid percussion model of experimental brain injury in the rat. *J. Neurosurg.* 67, 110–119.
- Fineman, I., Hovda, D.A., Smith, M., Yoshino, A., and Becker, D.P. (1993). Concussive brain injury is associated with a prolonged accumulation of calcium: a ^{45}Ca autoradiographic study. *Brain Res.* 624, 94–102.
- Foda, M.A., and Marmarou, A. (1994). A new model of diffuse brain injury in rats. Part II: Morphological characterization. *J. Neurosurg.* 80, 301–313.
- Geurts, A.C., Knoop, J.A., and van Limbeek, J. (1999). Is postural control associated with mental functioning in the persistent postconcussion syndrome? *Arch. Phys. Med. Rehabil.* 80, 144–149.
- Goda, M., Isono, M., Fujiki, M., and Kobayashi, H. (2002). Both MK801 and NBQX reduce the neuronal damage after impact-acceleration brain injury. *J. Neurotrauma* 19, 1445–1456.
- Hallam, T.M., Floyd, C.L., Folkerts, M.M., Lee, L.L., Gong, Q.Z., Lyeth, B.G., Muizelaar, J.P., and Berman, R.F. (2004). Comparison of behavioral deficits and acute neuronal degeneration in rat lateral fluid percussion and weight-drop brain injury models. *J. Neurotrauma* 21, 521–539.
- Hamm, R.J. (2001). Neurobehavioral assessment of outcome following traumatic brain injury in rats: an evaluation of selected measures. *J. Neurotrauma* 18, 1207–1216.
- Hamm, R.J., Temple, M.D., Pike, B.R., O'Dell, D.M., Buck, D.L., and Lyeth, B.G. (1996). Working memory deficits following traumatic brain injury in the rat. *J. Neurotrauma* 13, 317–323.
- Hicks, R.R., Smith, D.H., Lowenstein, D.H., Saint Marie, R., and McIntosh, T.K. (1993). Mild experimental brain injury in the rat induces cognitive deficits associated with regional neuronal loss in the hippocampus. *J. Neurotrauma* 10, 405–414.
- Hinton-Bayre, A.D., Geffen, G.M., Geffen, L.B., McFarland, K.A., and Friis, P. (1999). Concussion in contact sports: reliable change indices of impairment and recovery. *J. Clin. Exp. Neuropsychol.* 21, 70–86.
- Hoane, M.R., Knotts, A.A., Akstulewicz, S.L., Aquilano, M., and Means, L.W. (2003). The behavioral effects of magnesium therapy on recovery of function following bilateral anterior medial cortex lesions in the rat. *Brain Res. Bull.* 60, 105–114.
- Hovda, D.A., Yoshino, A., Kawamata, T., Katayama, Y., Fineman, I., and Becker, D.P. (1990). The increase in local cerebral glucose utilization following fluid percussion brain injury is prevented with kynurenic acid and is associated with an increase in calcium. *Acta Neurochir. Suppl. (Wien.)* 51, 331–333.
- Huh, J.W., Widing, A.G., and Raghupathi, R. (2008). Midline brain injury in the immature rat induces sustained cognitive deficits, bihemispheric axonal injury and neurodegeneration. *Exp. Neurol.* 213, 84–92.
- Katayama, Y., Becker, D.P., Tamura, T., and Ikezaki, K. (1990). Early cellular swelling in experimental traumatic brain injury: a phenomenon mediated by excitatory amino acids. *Acta Neurochir. Suppl. (Wien.)* 51, 271–273.
- Keene, C.S., and Bucci, D.J. (2009). Damage to the retrosplenial cortex produces specific impairments in spatial working memory. *Neurobiol. Learn. Mem.* 91, 408–414.
- Koo, E.H., Sisodia, S.S., Archer, D.R., Martin, L.J., Weidemann, A., Beyreuther, K., Fischer, P., Masters, C.L., and Price, D.L. (1990). Precursor of amyloid protein in Alzheimer disease undergoes fast anterograde axonal transport. *Proc. Natl. Acad. Sci. USA* 87, 1561–1565.
- Kraus, M.F., Susmaras, T., Caughlin, B.P., Walker, C.J., Sweeney, J.A., and Little, D.M. (2007). White matter integrity and cognition in chronic traumatic brain injury: a diffusion tensor imaging study. *Brain* 130, 2508–2519.
- Kumar, R., Husain, M., Gupta, R.K., Hasan, K.M., Haris, M., Agarwal, A.K., Pandey, C.M., and Narayana, P.A. (2009). Serial changes in the white matter diffusion tensor imaging metrics in moderate traumatic brain injury and correlation with neuro-cognitive function. *J. Neurotrauma* 26, 481–495.
- Laurer, H.L., Bareyre, F.M., Lee, V.M., Trojanowski, J.Q., Longhi, L., Hoover, R., Saatman, K.E., Raghupathi, R., Hoshino, S., Grady, M.S., and McIntosh, T.K. (2001). Mild head injury increasing the brain's vulnerability to a second concussive impact. *J. Neurosurg.* 95, 859–870.
- Levin, H.S., Mattis, S., Ruff, R.M., Eisenberg, H.M., Marshall, L.F., Tabaddor, K., High, W.M., Jr., and Frankowski, R.F. (1987). Neurobehavioral outcome following minor head injury: a three-center study. *J. Neurosurg.* 66, 234–243.
- Lewen, A., Li, G.L., Nilsson, P., Olsson, Y., and Hillered, L. (1995). Traumatic brain injury in rat produces changes of beta-amyloid precursor protein immunoreactivity. *Neuroreport* 6, 357–360.
- Longhi, L., Saatman, K.E., Fujimoto, S., Raghupathi, R., Meaney, D.F., Davis, J., McMillan, B.S.A., Conte, V., Laurer, H.L., Stein, S., Stocchetti, N., and McIntosh, T.K. (2005). Temporal window of vulnerability to repetitive experimental concussive brain injury. *Neurosurgery* 56, 364–374; discussion 364–374.
- Lovell, M., Collins, M., and Bradley, J. (2004). Return to play following sports-related concussion. *Clin. Sports Med.* 23, 421–441, ix.
- Lovell, M.R., Collins, M.W., Iverson, G.L., Field, M., Maroon, J.C., Cantu, R., Podell, K., Powell, J.W., Belza, M., and Fu, F.H. (2003). Recovery from mild concussion in high school athletes. *J. Neurosurg.* 98, 296–301.
- Lyeth, B.G., Jenkins, L.W., Hamm, R.J., Dixon, C.E., Phillips, L.L., Clifton, G.L., Young, H.F., and Hayes, R.L. (1990). Prolonged memory impairment in the absence of hippocampal cell death following traumatic brain injury in the rat. *Brain Res.* 526, 249–258.
- Maddocks, D., and Saling, M. (1996). Neuropsychological deficits following concussion. *Brain Inj.* 10, 99–103.
- Marmarou, C.R., Walker, S.A., Davis, C.L., and Povlishock, J.T. (2005). Quantitative analysis of the relationship between intra-axonal neurofilament compaction and impaired axonal transport following diffuse traumatic brain injury. *J. Neurotrauma* 22, 1066–1080.
- McCrea, M., Guskiewicz, K.M., Marshall, S.W., Barr, W., Randolph, C., Cantu, R.C., Onate, J.A., Yang, J., and Kelly, J.P. (2003). Acute effects and recovery time following concussion in collegiate football players: the NCAA Concussion Study. *JAMA* 290, 2556–2563.
- McCrory, P., Meeuwisse, W., Johnston, K., Dvorak, J., Aubry, M., Molloy, M., and Cantu, R. (2009). Consensus statement on concussion in sport—the Third International Conference on

- Concussion in Sport held in Zurich, November 2008. *Phys. Sportsmed.* 37, 141–159.
- Milman, A., Rosenberg, A., Weizman, R., and Pick, C.G. (2005). Mild traumatic brain injury induces persistent cognitive deficits and behavioral disturbances in mice. *J. Neurotrauma* 22, 1003–1010.
- Miyazaki, S., Katayama, Y., Lyeth, B.G., Jenkins, L.W., DeWitt, D.S., Goldberg, S.J., Newlon, P.G., and Hayes, R.L. (1992). Enduring suppression of hippocampal long-term potentiation following traumatic brain injury in rat. *Brain Res.* 585, 335–339.
- Niogi, S.N., Mukherjee, P., Ghajar, J., Johnson, C., Kolster, R.A., Sarkar, R., Lee, H., Meeker, M., Zimmerman, R.D., Manley, G.T., and McCandliss, B.D. (2008). Extent of microstructural white matter injury in postconcussive syndrome correlates with impaired cognitive reaction time: a 3T diffusion tensor imaging study of mild traumatic brain injury. *AJNR Am. J. Neuroradiol.* 29, 967–973.
- Ohlsson, M., Mattsson, P., and Svensson, M. (2004). A temporal study of axonal degeneration and glial scar formation following a standardized crush injury of the optic nerve in the adult rat. *Restor. Neurol. Neurosci.* 22, 1–10.
- Oppenheimer, D.R. (1968). Microscopic lesions in the brain following head injury. *J. Neurol. Neurosurg. Psychiatry* 31, 299–306.
- Papp, H., Pakaski, M., and Kasa, P. (2002). Presenilin-1 and the amyloid precursor protein are transported bidirectionally in the sciatic nerve of adult rat. *Neurochem. Int.* 41, 429–435.
- Phillips, L.L., Lyeth, B.G., Hamm, R.J., and Povlishock, J.T. (1994). Combined fluid percussion brain injury and entorhinal cortical lesion: a model for assessing the interaction between neuroexcitation and deafferentation. *J. Neurotrauma* 11, 641–656.
- Pothuizen, H.H., Davies, M., Aggleton, J.P., and Vann, S.D. (2010). Effects of selective granular retrosplenial cortex lesions on spatial working memory in rats. *Behav. Brain Res.* 208, 566–575.
- Povlishock, J.T., Becker, D.P., Cheng, C.L., and Vaughan, G.W. (1983). Axonal change in minor head injury. *J. Neuropathol. Exp. Neurol.* 42, 225–242.
- Povlishock, J.T., Marmarou, A., McIntosh, T., Trojanowski, J.Q., and Moroi, J. (1997). Impact acceleration injury in the rat: evidence for focal axolemmal change and related neurofilament sidearm alteration. *J. Neuropathol. Exp. Neurol.* 56, 347–359.
- Reeves, T.M., Phillips, L.L., and Povlishock, J.T. (2005). Myelinated and unmyelinated axons of the corpus callosum differ in vulnerability and functional recovery following traumatic brain injury. *Exp. Neurol.* 196, 126–137.
- Reeves, T.M., Zhu, J., Povlishock, J.T., and Phillips, L.L. (1997). The effect of combined fluid percussion and entorhinal cortical lesions on long-term potentiation. *Neuroscience* 77, 431–444.
- Ropper, A.H., and Gorson, K.C. (2007). Clinical practice. Concussion. *N. Engl. J. Med.* 356, 166–172.
- Ryan, L.M., and Warden, D.L. (2003). Post concussion syndrome. *Int. Rev. Psychiatry.* 15, 310–316.
- Saatman, K.E., Abai, B., Grosvenor, A., Vorwerk, C.K., Smith, D.H., and Meaney, D.F. (2003). Traumatic axonal injury results in biphasic calpain activation and retrograde transport impairment in mice. *J. Cereb. Blood Flow Metab.* 23, 34–42.
- Saatman, K.E., Feeko, K.J., Pape, R.L., and Raghupathi, R. (2006). Differential behavioral and histopathological responses to graded cortical impact injury in mice. *J. Neurotrauma* 23, 1241–1253.
- Schalomon, P.M., and Wahlsten, D. (1995). A precision surgical approach for complete or partial callosotomy in the mouse. *Physiol. Behav.* 57, 1199–1203.
- Schmued, L.C., Albertson, C., and Slikker, W., Jr. (1997). Fluoro-Jade: a novel fluorochrome for the sensitive and reliable histochemical localization of neuronal degeneration. *Brain Res.* 751, 37–46.
- Schmued, L.C., and Fallon, J.H. (1986). Fluoro-Gold: a new fluorescent retrograde axonal tracer with numerous unique properties. *Brain Res.* 377, 147–154.
- Shoji, H., and Kibayashi, K. (2006). Changes in localization of synaptophysin following fluid percussion injury in the rat brain. *Brain Res.* 1078, 198–211.
- Smits, M., Houston, G.C., Dippel, D.W., Wielopolski, P.A., Vernooij, M.W., Koudstaal, P.J., Hunink, M.G., and van der Lugt, A. (2010). Microstructural brain injury in post-concussion syndrome after minor head injury. *Neuroradiology* [Epub ahead of print].
- Spain, A., Dumas, S., Lifshitz, J., Rhodes, J., Andrews, P.J., Horsburgh, K., and Fowler, J.H. (2010). Mild fluid percussion injury in mice produces evolving selective axonal pathology and cognitive deficits relevant to human brain injury. *J. Neurotrauma* 27, 1429–1438.
- Stone, J.R., Singleton, R.H., and Povlishock, J.T. (2000). Antibodies to the C-terminus of the beta-amyloid precursor protein (APP): a site specific marker for the detection of traumatic axonal injury. *Brain Res.* 871, 288–302.
- Tang, Y.P., Noda, Y., Hasegawa, T., and Nabeshima, T. (1997a). A concussive-like brain injury model in mice (I): impairment in learning and memory. *J. Neurotrauma* 14, 851–862.
- Tang, Y.P., Noda, Y., Hasegawa, T., and Nabeshima, T. (1997b). A concussive-like brain injury model in mice (II): selective neuronal loss in the cortex and hippocampus. *J. Neurotrauma* 14, 863–873.
- Tashlykov, V., Katz, Y., Gazit, V., Zohar, O., Schreiber, S., and Pick, C.G. (2007). Apoptotic changes in the cortex and hippocampus following minimal brain trauma in mice. *Brain Res.* 1130, 197–205.
- Tong, W., Igarashi, T., Ferriero, D.M., and Noble, L.J. (2002). Traumatic brain injury in the immature mouse brain: characterization of regional vulnerability. *Exp. Neurol.* 176, 105–116.
- Tweedie, D., Milman, A., Holloway, H.W., Li, Y., Harvey, B.K., Shen, H., Pistell, P.J., Lahiri, D.K., Hoffer, B.J., Wang, Y., Pick, C.G., and Greig, N.H. (2007). Apoptotic and behavioral sequelae of mild brain trauma in mice. *J. Neurosci. Res.* 85, 805–815.
- Wiedenmann, B., and Franke, W.W. (1985). Identification and localization of synaptophysin, an integral membrane glycoprotein of Mr 38,000 characteristic of presynaptic vesicles. *Cell* 41, 1017–1028.
- Wilde, E.A., McCauley, S.R., Hunter, J.V., Bigler, E.D., Chu, Z., Wang, Z.J., Hanten, G.R., Troyanskaya, M., Yallampalli, R., Li, X., Chia, J., and Levin, H.S. (2008). Diffusion tensor imaging of acute mild traumatic brain injury in adolescents. *Neurology* 70, 948–955.
- Williams, W.H., Potter, S., and Ryland, H. (2010). Mild traumatic brain injury and postconcussion syndrome: a neuropsychological perspective. *J. Neurol. Neurosurg. Psychiatry* 81, 1116–1122.
- Wozniak, J.R., Krach, L., Ward, E., Mueller, B.A., Muetzel, R., Schnoebelen, S., Kiragu, A., and Lim, K.O. (2007). Neurocognitive and neuroimaging correlates of pediatric traumatic brain injury: a diffusion tensor imaging (DTI) study. *Arch. Clin. Neuropsychol.* 22, 555–568.

- Yamaki, T., Murakami, N., Iwamoto, Y., Sakakibara, T., Kobori, N., Ueda, S., Kikuchi, T., and Uwahodo, Y. (1997). Evaluation of learning and memory dysfunction and histological findings in rats with chronic stage contusion and diffuse axonal injury. *Brain Res.* 752, 151–160.
- Yamaki, T., Murakami, N., Iwamoto, Y., Yoshino, E., Nakagawa, Y., Ueda, S., Horikawa, J., and Tsujii, T. (1994). A modified fluid percussion device. *J. Neurotrauma* 11, 613–622.
- Yoshino, A., Hovda, D.A., Kawamata, T., Katayama, Y., and Becker, D.P. (1991). Dynamic changes in local cerebral glucose utilization following cerebral conclusion in rats: evidence of a hyper- and subsequent hypometabolic state. *Brain Res.* 561, 106–119.
- Zohar, O., Schreiber, S., Getslev, V., Schwartz, J.P., Mullins, P.G., and Pick, C.G. (2003). Closed-head minimal traumatic brain injury produces long-term cognitive deficits in mice. *Neuroscience* 118, 949–955.

Address correspondence to:

Ramesh Raghupathi, Ph.D.

Drexel University College of Medicine

Department of Neurobiology and Anatomy

2900 Queen Lane, Room 277

Philadelphia, PA 19129

E-mail: RRamesh@drexelmed.edu

